Buckling and supercritical behavior of axially moving plates

Yury Vetyukov
yury.vetyukov@tuwien.ac.at

Abstract

We consider a flexible plate moving across a domain, bounded by two parallel lines. Velocities of the plate, with which it is entering the domain and leaving it, are kinematically prescribed and may vary in space and time. The deformation of the plate is quasistatically analyzed using the geometrically nonlinear model of a Kirchhoff shell with a mixed Eulerian-Lagrangian kinematic description. In contrast to the formulations, available in the literature, neither the in-plane nor the out-of-plane deformations are unknown a priori and may be arbitrarily large. The particles of the plate travel across a finite element mesh, which remains fixed in the axial direction. The evident advantage of the approach is that the boundary conditions need to be applied at fixed edges of the finite elements. In the paper, we present the mathematical formulation and demonstrate its consistency by comparing the solution of a benchmark problem against results, obtained with conventional Lagrangian finite elements.

1 Introduction

The problem of mathematical modeling of nonlinear deformations of axially moving structures is both challenging and practically important. Numerous papers deal with the transverse vibrations of axially moving beams and strings, see a review paper by Chen, Ref. [1]. While an extension towards nonlinearly coupled in-plane and out-of-plane vibrations of a moving plate is presented in Ref. [5], this model is incapable of representing arbitrarily deformed configurations of the plate. Moreover, the use of Lagrange equations of motion to an open system with influx and outflux of the mass is not justified by the authors of the latter reference.

Large axial deformation and bending of a beam, which can move across a fixed domain, is treated by Humer and Irschik in Ref. [6] using a suitable change of variables. We apply a similar technique for the quasistatic modeling of finite deformations of a plate, which is moving across a given domain in the direction $\mathtt{x}$. The velocities of the plate are prescribed at two boundaries of the domain $\mathtt{x} = 0$ and $\mathtt{x} = \mathtt{L}$, see Fig. 1. Rolling of metal strips, paper production or motion of conveyor belt are a few examples of mechanical engineering problems, which can make use of model at hand. Non-constant profiles of the velocities, with which the particles of the plate are entering the domain $v_{\mathrm{entry}}(\mathtt{y})$ and leaving it $v_{\mathrm{exit}}(\mathtt{y})$, lead to the

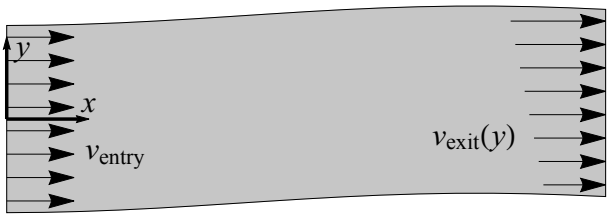

Figure 1: Deformation of a plate with prescribed velocities at the boundaries

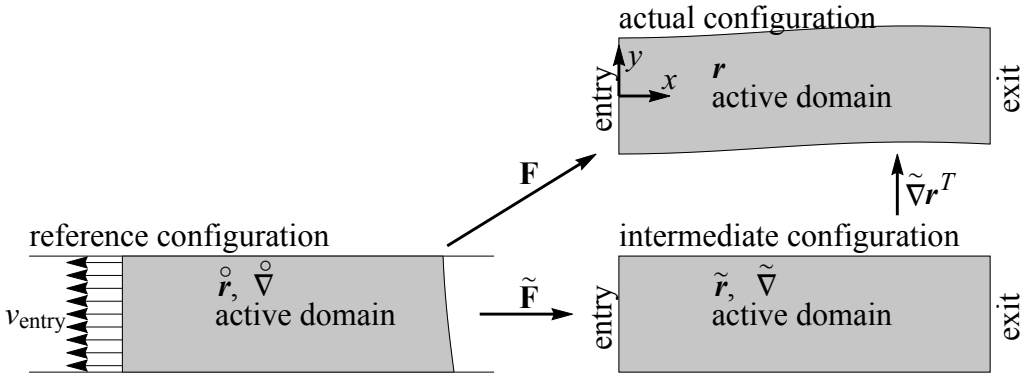

Figure 2: Two-stage mapping from the reference configuration to the actual one: the intermediate configuration is fixed in space

in-plane deformations. For thin plates this results in various forms of out-of-plane buckling. Accurate simulations using conventional Lagrangian finite element models are difficult because the boundaries of the domain cross the finite element mesh and kinematic boundary conditions need to be imposed inside the elements. The problem is getting even more prominent as the finite element simulations are coupled with a closed-loop control scheme, which is important for practical applications.

2 Mathematical model

In the present study we assume the velocity v_{entry}, with which the plate is entering the domain, to be constant. In the future, arbitrary velocity profiles may be incorporated into the model by using the notion of intrinsic strains and the technique of multiplicative decomposition of the deformation gradient, see Ref. [7]. The varying velocity profile $v_{\text{exit}}(y)$, with which the material particles of the plate are leaving the domain at $x = L$, leads to the time varying deformation. Seeking a sequence of quasistatic equilibrium states of the elastic structure, we need to minimize the total energy of the active region of the plate, which is currently residing in the considered domain. Not going into details concerning the time integration, which is intended to be discussed in future publications, we focus on the kinematic modeling of the deformation of the plate.

The plane reference configuration $0 \le \mathring{y} \le w$ is straight (w is the undeformed

width and $\mathring{\mathbf{r}} = \mathring{x}\mathbf{i} + \mathring{y}\mathbf{j}$ is the position vector in the reference configuration), see Fig. 2. The present mixed Eulerian-Lagrangian kinematic description makes use of a fixed intermediate configuration with the position vector $\tilde{\mathbf{r}}$ such, that the mapping of the positions of particles from the reference configuration to the actual one $\mathbf{r} = \mathbf{r}(\mathring{\mathbf{r}})$ comprises two stages:

$$\begin{aligned} \tilde{\mathbf{r}} &= \mathring{\mathbf{r}} + u_x(\tilde{\mathbf{r}})\mathbf{i}, \\ \mathbf{r} &= \tilde{\mathbf{r}} + u_y(\tilde{\mathbf{r}})\mathbf{j} + u_z(\tilde{\mathbf{r}})\mathbf{k}. \end{aligned} \tag{1}$$

Simplicity of this description essentially distinguishes it from the known Arbitrary Lagrangian-Eulerian formulation, Ref. [2]: neither re-meshing nor transport of mechanical fields between the time steps are required. All fields are functions of the place in the fixed intermediate configuration, in which a finite element discretization of the field of displacements $\mathbf{u} = u_x\mathbf{i} + u_y\mathbf{j} + u_z\mathbf{k}$ is performed.

We apply the classical Kirchhoff model of a shell with five degrees of freedom of particles, see Refs. [3, 4, 8]. Expressions for the strain measures require the gradient of deformation of the plate from the reference configuration to the actual one

$$\mathbf{F} = \mathring{\nabla}\mathbf{r}^{\mathsf{T}}, \tag{2}$$

in which

$$\mathring{\nabla} = \mathbf{i}\frac{\partial}{\partial \mathring{x}} + \mathbf{j}\frac{\partial}{\partial \mathring{y}} \tag{3}$$

is the differential operator of the reference state. As the finite element discretization is performed in the intermediate configuration, we need to express $\mathbf{F}$ using the corresponding differential operator

$$\tilde{\nabla} = \mathbf{i}\frac{\partial}{\partial \tilde{x}} + \mathbf{j}\frac{\partial}{\partial \tilde{y}} = \mathbf{i}\frac{\partial}{\partial x} + \mathbf{j}\frac{\partial}{\partial \mathring{y}}, \tag{4}$$

the axial coordinate in the intermediate configuration $\tilde{x}$ equals the actual one, and the transverse coordinate $\tilde{y}$ equals the reference one according to (1). Now, the two differential operators are related by the gradient of deformation from the reference configuration to the intermediate one $\tilde{\mathbf{F}}$:

$$\mathring{\nabla} = \tilde{\mathbf{F}}^{\mathsf{T}} \cdot \tilde{\nabla}, \quad \tilde{\mathbf{F}}^{\mathsf{T}} = \mathring{\nabla}\tilde{\mathbf{r}}^{\mathsf{T}}. \tag{5}$$

Finally, total gradient of deformation of the plate with the differential operator of the intermediate configuration $\tilde{\nabla}$ results in the form

$$\begin{aligned} \mathbf{F} &= \mathring{\nabla}\mathbf{r}^{\mathsf{T}} = \tilde{\nabla}\mathbf{r}^{\mathsf{T}} \cdot \tilde{\mathbf{F}}, \\ \tilde{\mathbf{F}} &= \left(\mathbf{I}_2 - \mathbf{i}\tilde{\nabla}u_x\right)^{-1}. \end{aligned} \tag{6}$$

Here $\mathbf{I}_2 = \mathbf{ii} + \mathbf{jj}$ is the in-plane identity tensor, and the expression for the in-plane tensor $\tilde{\mathbf{F}}$ follows from

$$\mathbf{I}_2 = \mathring{\nabla}\mathring{\mathbf{r}} = \tilde{\mathbf{F}}^{\mathsf{T}} \cdot \tilde{\nabla}(\tilde{\mathbf{r}} - u_x\mathbf{i}). \tag{7}$$

The strain measures of a classical shell

$$\begin{aligned} \mathbf{E} &= \frac{1}{2}\left(\mathbf{F}^{\mathsf{T}}\cdot\mathbf{F}-\mathbf{I}_2\right), \\ \mathbf{K} &= \mathbf{F}^{\mathsf{T}}\cdot\mathbf{b}\cdot\mathbf{F} \end{aligned} \tag{8}$$

feature the actual second metric tensor $\mathbf{b} = -\nabla\mathbf{n}$, in which $\mathbf{n}$ is the vector of unit normal and $\nabla = \mathbf{F}^{\mathsf{T}}\cdot\overset{\circ}{\nabla}$ is the differential operator on the deformed surface. After mathematical transformations we express the tensor of bending strains with the operator of the intermediate configuration:

$$\mathbf{K} = \tilde{\mathbf{F}}^{\mathsf{T}}\cdot\tilde{\mathbf{K}}\cdot\tilde{\mathbf{F}}, \quad \tilde{\mathbf{K}} = \tilde{\nabla}\tilde{\nabla}\mathbf{r}\cdot\mathbf{n}. \tag{9}$$

Here we restrict the analysis to pure elastic material behavior. The strain energy of the plate per unit area in the reference configuration is computed as a quadratic form

$$U = \frac{1}{2}\left(A_1(\operatorname{tr}\mathbf{E})^2 + A_2\mathbf{E}\cdot\cdot\mathbf{E} + D_1(\operatorname{tr}\mathbf{K})^2 + D_2\mathbf{K}\cdot\cdot\mathbf{K}\right) \tag{10}$$

with known coefficients, see Refs. [4, 8]. The total strain energy

$$U^{\Sigma} = \int_0^L \int_{-w/2}^{w/2} U(\det\tilde{\mathbf{F}})^{-1}\mathrm{d}\tilde{y}\,\mathrm{d}x \tag{11}$$

is integrated in the intermediate configuration using the finite element discretization of displacements $\mathbf{u}$ and minimized at each time step of the quasistatic simulation. As discussed after (16), known velocities of particles v_{entry} and v_{exit} determine the time variations of the axial displacements u_x at the boundaries $x = 0$ and $x = L$, which means that the material volume of the active domain is prescribed for each time step. This allows seeking static equilibrium configurations by minimizing the total strain energy of this material volume, which is changing during the simulation, but is known for each time step.

3 Time stepping scheme

In a numerical simulation, we discretize the evolution of the system in time and need to formulate an algorithm of transformation of the solution from one time step t^k to the next one $t^{k+1} = t^k + \tau$. In the beginning of a time step, the field of displacements $\mathbf{u}^k(\tilde{\mathbf{r}})$ is known in the form of a finite element approximation. Now, each particular material point moves with the velocity $\dot{\mathbf{u}}$, in which the full time derivative is defined for a fixed material particle as

$$(\ldots)^{\cdot} \equiv \left.\frac{\partial\ldots}{\partial t}\right|_{\overset{\circ}{\mathbf{r}}=\text{const}}. \tag{12}$$

The notion of a local time derivative with fixed $\tilde{\mathbf{r}}$ is relevant for the description in the intermediate configuration:

$$\partial_t(\ldots) \equiv \left.\frac{\partial\ldots}{\partial t}\right|_{\tilde{\mathbf{r}}=\text{const}}. \tag{13}$$

The transformation between the full and the local time derivatives can be easily derived by considering a field $\mathbf{u}(\tilde{\mathbf{r}}, t)$, which is defined in the intermediate configuration. Computing $\dot{\mathbf{u}}$, we take into account that $\tilde{\mathbf{r}} = \tilde{\mathbf{r}}(\mathring{\mathbf{r}}, t)$ changes in time for $\mathring{\mathbf{r}} = \text{const}$, and arrive at

$$\dot{\mathbf{u}} = \partial_t \mathbf{u} + \dot{\tilde{\mathbf{r}}} \cdot \tilde{\nabla} \mathbf{u}. \tag{14}$$

Using the first relation in (1) and taking into account that the full time derivative $\mathring{\dot{\mathbf{r}}} = 0$, we find

$$\dot{\mathbf{u}} = \partial_t \mathbf{u} + \dot{u}_x \mathbf{i} \cdot \tilde{\nabla} \mathbf{u} = \partial_t \mathbf{u} + \dot{u}_x \partial_x \mathbf{u}. \tag{15}$$

This results in

$$\dot{u}_x = \partial_t u_x \left(1 - \partial_x u_x\right)^{-1}. \tag{16}$$

The definitions of material and local time derivatives are used to formulate a strategy for the time stepping. Neglecting the dynamic effects, we consider the time evolution of the deformation of the plate owing to the prescribed velocities at the boundaries of the domain. Seeking for an equilibrium state at each time step, we minimize the total strain energy of the active domain U^{Σ}. Although the material of the plate is flowing across the intermediate configuration, this approach is justified as the material volume within the active domain is fixed for the end of the time step. Indeed, according to the boundary conditions, discussed below, the displacements at the two boundaries of the domain (19) are known for the end of the time step $t = t^{k+1}$. This means that the boundaries of the active domain in the reference configuration are fixed according to the first relation in (1), and seeking the equilibrium of this material volume is equivalent to minimizing its total energy.

4 Boundary conditions at a time step

In this section, we discuss the time evolution of the displacements of the plate at the boundaries of the domain $x = 0$ and $x = L$. We interpret the velocity at the entry to the active domain v_{entry} as the time rate of material generation. This is relevant e.g. for modeling rolling processes, in which the time rate of the material volume flowing across a roll gap is known. Owing to the deformation, the particles acquire a different material velocity after entering the active domain. In contrast, v_{exit} is the material velocity, with which the particles of the plate leave the domain at the entry to the subsequent roll gap.

The analysis in the present paper is restricted to a particular case of constant entry velocity. The left boundary of the intermediate configuration moves across the reference one to the left with $v_{\text{entry}} = \text{const}$, which means that an infinitesimally thin layer of the plate with the length $v_{\text{entry}} dt$ enters the active domain during the time dt. The local time derivatives here are known:

$$x = 0: \quad \partial_t \mathring{\mathbf{r}} = -v_{\text{entry}} \mathbf{i}, \quad \partial_t \tilde{\mathbf{r}} = 0; \quad (1) \quad \Rightarrow \quad \partial_t \mathbf{u} = v_{\text{entry}} \mathbf{i}. \tag{17}$$

We immediately conclude that $u_x = v_{\text{entry}} t$ and $v_y = 0$ at the left boundary.

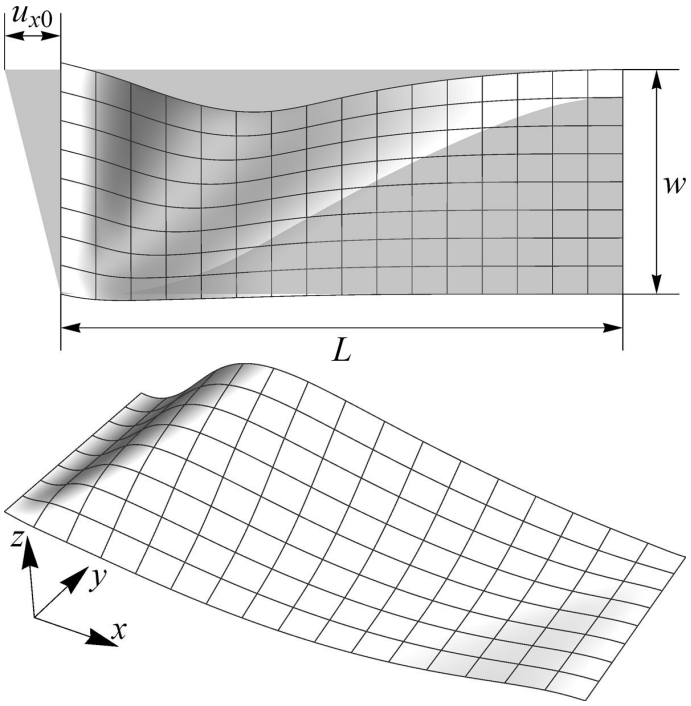

Figure 3: Deformation of a trapezoidal plate, seen from above (together with the undeformed configuration) and from the side

At the right boundary we know material velocities, and the local time derivatives follow:

$$x = L: \quad \dot{\mathbf{u}} = v_{\text{exit}}\mathbf{i}; \quad (15) \quad \Rightarrow \quad \partial_t \mathbf{u} = v_{\text{exit}}(\mathbf{i} - \partial_x \mathbf{u}). \tag{18}$$

It is important to notice, that although the material time derivative here is always directed along x, the line of contact would still travel in the transverse direction because $\partial_t \mathbf{u} \cdot \mathbf{j} \neq 0$ as long as the plate is inclined and $\partial_x u_y \neq 0$.

In the beginning of a time step $t = t^k$, the local time derivatives $\partial_t \mathbf{u}$ are available at the boundaries $x = 0$ and $x = L$. Experience shows, that an explicit time integration scheme for the boundary conditions with a moderately small time step size τ leads to accurate simulation results, which rapidly converge as $\tau \to 0$:

$$x = 0, L: \quad \mathbf{u}^{k+1} = \mathbf{u}^k + \tau\, \partial_t \mathbf{u}. \tag{19}$$

5 Numerical benchmark problem

While the results of numerical modeling of deformation of axially moving plates will be reported in future publications, here we test the formulation by seeking the equilibrium of a trapezoidal plate of the width w and side lengths L and $L + u_{x0}$, see Fig. 3. The inclined edge is rotated parallel to the right one by kinematically prescribed displacements u_x and u_y such, that the actual configuration is bounded by the lines $x = 0$ and $x = L$; the length of the edge is preserved constant to

Table 1: Mesh convergence and comparison of the mixed Eulerian-Lagrangian and traditional Lagrangian frameworks

Discretization,	Mixed E.-L.		Lagrangian	
$n_x \times n_y$	$\min u_z$	$\max u_z$	$\min u_z$	$\max u_z$
4×2	-0.07270	0.18577	-0.07322	0.18138
8×4	-0.05846	0.18427	-0.05831	0.18256
16×8	-0.05542	0.18319	-0.05527	0.18259
32×16	—	—	-0.05490	0.18262

avoid large in-plane strains. The mapping (1) is thus possible with the intermediate configuration $0 \leq x \leq L$, $0 \leq \tilde{y} \leq w$, which is discretized using C^1 continuous finite element approximation of displacements, presented by the author in Refs. [8, 9].

The compressed shell buckles out of plane, and the region with $u_z < 0$ is "shadowed" by the gray initial configuration in Fig. 3. The transverse edges of the finite element mesh remain parallel in the deformed configuration. This corresponds to the second relation in (1), as the mapping $\mathbf{r}(\tilde{\mathbf{r}})$ features only u_y and u_z.

The considered parameters of the model in SI system are $L = 1$, $w = 0.4$, thickness of the plate $5 \cdot 10^{-3}$, Young modulus $2.1 \cdot 10^{11}$ and Poisson ratio 0.3. In Table 1 we summarized the maximal and minimal values of the out-of-plane displacements, computed for various discretizations using the present method as well as the conventional shell finite elements with Lagrangian description, discussed in the above references. These maximal and minimal displacements take place at the opposite edges of the plate. We initiated out-of-plane displacements by applying and then releasing a transverse distributed load in the positive direction of z axis, which determined the direction of buckling in all simulations. The current implementation of the mixed Eulerian-Lagrangian finite element formulation using *Wolfram Mathematica* is yet restricted concerning the size of the mesh, but one can conclude that the results converge to the same solution.

Acknowledgements

This work has been partially carried out at LCM GmbH as part of a K2 project. K2 projects are financed using funding from the Austrian COMET-K2 programme. The COMET K2 projects at LCM are supported by the Austrian federal government, the federal state of Upper Austria, the Johannes Kepler University and all of the scientific partners which form part of the K2-COMET Consortium.

References

[1] Chen, L.-Q., Analysis and control of transverse vibrations of axially moving strings, *Appl Mech Rev*, 58, pp. 91-116, 2005.

[2] Donea, J., Huerta, A., Ponthot, J.-P. and Rodriguez-Ferran, A., *Arbitrary Lagrangian-Eulerian methods*, in *Encyclopedia of Computational Mechanics*,

vol. 1: Fundamentals, Stein, E., de Borst, R. and Hughes, T. (eds.), chap. 14, John Wiley & Sons, Ltd, 2004.

[3] Eliseev, V., *Mechanics of deformable solid bodies* (in Russian). St.Petersburg State Polytechnical University Publishing House, 2006

[4] Eliseev, V. and Vetyukov, Y., Finite deformation of thin shells in the context of analytical mechanics of material surfaces, *Acta Mech*, 209, pp. 43-57, 2010.

[5] Ghayesh, M. H., Amabili, M. and Païdoussis, M. P., Nonlinear dynamics of axially moving plates, *J Sound Vib*, 332, pp. 391-406, 2013.

[6] Humer, A. and Irschik, H., Large deformation and stability of an extensible elastica with an unknown length, *Int J Solids Struct*, 48, pp. 1301-1310, 2011.

[7] Humer, A. and Krommer, M., Modeling of piezoelectric materials by means of a multiplicative decomposition of the deformation gradient, *Mech Adv Mat Struc*, 22, pp. 125-135, 2015.

[8] Vetyukov, Y., *Nonlinear Mechanics of thin-walled structures. Asymptotics, direct approach and numerical analysis*, Springer, Vienna, 2014.

[9] Vetyukov, Y., Finite element modeling of Kirchhoff-Love shells as smooth material surfaces, *ZAMM*, 94, pp. 150-163, 2014.

Yury Vetyukov, Institute of Mechanics and Mechatronics, Vienna University of Technology, Getreidemarkt 9, 1060 Vienna, Austria